

A novel kind of nitrogen heterocycle compound induces apoptosis of human chronic myelogenous leukemia K562 cells

Guoyu Ding,^{a,b} Feng Liu,^a Ting Yang,^b Yuyang Jiang,^{a,b,*} Hua Fu^b and Yufen Zhao^b

^aKey Laboratory of Chemical Biology, Guangdong Province, Graduate School of Shenzhen, Tsinghua University, Shenzhen 518057, PR China

^bKey Laboratory of Bioorganic Phosphorus Chemistry and Chemical Biology, Ministry of Education, Department of Chemistry, Tsinghua University, Beijing 100084, PR China

Received 6 December 2005; revised 13 January 2006; accepted 14 January 2006
Available online 8 February 2006

Abstract—The effects of a novel kind of nitrogen heterocycle compound, which was synthesized in our laboratory previously, on human chronic myelogenous leukemia K562 cells were investigated. The morphological changes were observed by Acridine orange (AO) staining. The screened results through DNA fragmentation and the Annexin V-FITC/PI staining assay showed that compound **8** blocked cell cycles at G₁ phase which led to apoptosis. The increase of caspase-3, 8, and 9 was detected, indicating that both of death-receptor and mitochondria-pathways were activated. Compound **8** induced a biphasic alteration in mitochondrial membrane potential of K562 cells. A dramatic elevation of Ca²⁺ was also observed. In addition, a transient increase of ROS was also involved in the process. This study showed that compound **8** might be a potential chemopreventive agent for chronic myelogenous leukemia. It would guide our future work to synthesize more compounds derived from compound **8**, which might have better effect, and to determine the target protein. Moreover, it might also provide a background mechanism for the introduction of this new type of promising therapeutic agent.

© 2006 Elsevier Ltd. All rights reserved.

1. Introduction

Apoptosis is essential for normal development and the maintenance of homeostasis. It is involved in a variety of clinical disorders such as cancer, autoimmunity, hematopoietic disorders, and infertility. Many current anticancer drugs kill particular types of tumor cells through apoptosis. Apoptotic cells are characterized by specific morphological and biochemical changes, including cell shrinkage, chromatin condensation, budding, and internucleosomal cleavage of genomic DNA. The process is tightly regulated and mainly orchestrated by a family of cysteine proteases called caspases.^{1–3} Two main apoptosis pathways have been identified, the death-receptor pathway and the mitochondrial pathway. The death-receptor pathway is triggered through ligands binding to receptors in the plasma membrane, such as the Fas/CD95 and TNFR1, which subsequently

activate caspase-8 and downstream caspases. The mitochondrial pathway involves the activation of caspase-9 which in turn activates downstream executioners.^{4–6} They are responsible for a variety of key events in apoptotic process, such as changes in electron transport, loss of mitochondrial transmembrane potential (MMP, $\Delta\Psi_m$), failure of Ca²⁺ control, generation of reactive oxygen species (ROS), and the participation of pro- (such as Bax) and anti-apoptotic (such as Bcl-2 and Bcl-x_L) Bcl-2 family proteins.⁷ However, both of the two pathways converge at the level of caspase-3 activation, resulting in chromosomal DNA fragmentation.⁸

Medium-sized heterocycles are very important compounds as biologically active natural products⁹ and drug candidates,¹⁰ and benzolactams showed the anticancer effects on diverse tumor cells.^{11,12} In our previous research, diisopropylphosphoryl (DIPP) dipeptide (DIPP-L-Leu)₂-L-LysOCH₃ was found to induce apoptosis of Human Leukemia K562 cell, and phosphoryl played an important role, so we designed the medium- and large-sized nitrogen heterocycles containing diisopropylphosphoryl (compounds **1–14** in Table 1) to induce apoptosis of human chronic myelogenous

Keywords: Nitrogen heterocycle compounds; K562 cell apoptosis; Caspase-3,8,9; G₁ arrest.

* Corresponding author. Tel.: +86 10 6278 9262; fax: +86 10 6278 1695; e-mail: jiangyuy@mail.tsinghua.edu.cn

Table 1. IC₅₀ of the synthesized compounds against K562 cells

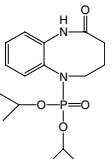
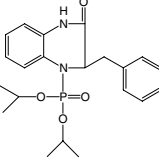
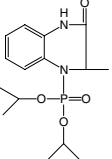
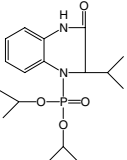
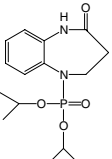
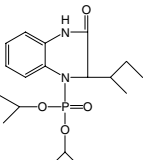
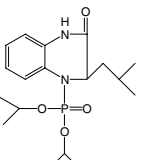
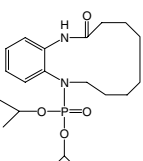
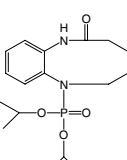
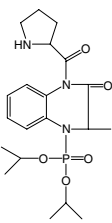
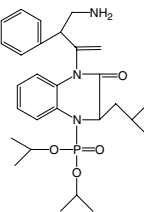
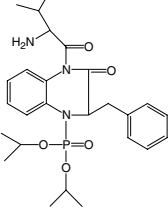
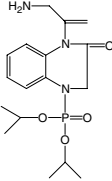
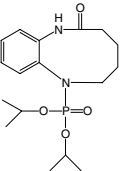
No.	Compound	IC ₅₀ (μg/mL)
1		>100
2		81.58
3		>100
4		>100
5		>100
6		92.51
7		>100
8		20.83
9		>100

Table 1 (continued)

No.	Compound	IC ₅₀ (μg/mL)
10		>100
11		>100
12		>100
13		>100
14		>100

leukemia K562 cells, and the target compounds were prepared via copper-catalyzed intramolecular N-arylation of phosphoramidates.¹³

Concerning our attractive novel nitrogen heterocycle compounds, it is necessary to study their pharmacological mode of action at cellular and molecular levels. The present study is to investigate the antiproliferative effects of these compounds on human chronic myelogenous leukemia (CML) K562 cells through screening the best inducer and then proving its machinery. Our results showed that compound **8** inhibited proliferation via blocking cell cycle progression at G₁ phase and subsequently progressing into apoptosis. Both death-receptor and mitochondrial pathways are activated. The underlying events relevant to mitochondria were studied in detail, including the alteration of MMP, ROS generation, and failure control of Ca²⁺ homeostasis.

2. Results and discussion

2.1. Inhibition of K562 growth induced by the synthesized compounds

K562 cells were treated with compounds **1–14** at a concentration of 100 $\mu\text{g/mL}$ and MTT was used to assay if the compounds have antiproliferative effects. Among the 14 compounds, compound **8** has the lowest IC_{50} (inhib-

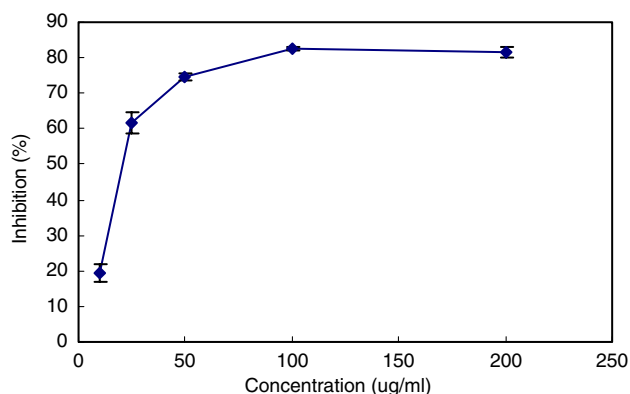


Figure 1. Effect of compound **8** on the inhibition of K562 cells. The cells were treated with compound **8** at the indicated concentrations for 24 h. The inhibition was determined by MTT assay. Each point is the mean of three replicates; bars represent the standard deviation.

Table 2. IC_{50} of compound **8** on CNE1, CNE2, HeLa, and MCF-7 cells at 24 h

Tumor cells	IC_{50} ($\mu\text{g/mL}$)
CNE1	19.25
CNE2	14.10
HeLa	23.96
MCF-7	10.78

itory concentration 50%), 20.83 $\mu\text{g/mL}$, and displayed the most potent inhibition activity, so it was used as the inducer in the following assays (Fig. 1). In addition, compound **8** can also inhibit the growth of other tumor cells, such as CNE1, CNE2, HeLa, and MCF-7. The results by MTT assay are shown in Table 2.

2.2. Compound **8** induces G_1 arrest and apoptosis in K562 cells

Figure 2A shows the representative morphology of K562 cells when exposed to compound **8** for 24 h, whereas the control K562 cells appeared normal features, with the nuclei round and homogeneous. After treatment, the cells exhibited the characteristic features of apoptosis, such as the appearance of apoptotic bodies, chromatin condensation, and fragmentation, as indicated by Acridine orange (AO) staining. In addition, the treated cells showed somewhat smaller than control cells in cellular size. The distribution of cell cycle was examined at the indicated times. At a concentration of 50 $\mu\text{g/mL}$, compound **8** induced a time-dependent increase of G_1 cell population in K562 cells from 44.46% at 8 h to 65.78% at 24 h (Fig. 2C). A biochemical hallmark of apoptosis is the fragmentation of genomic DNA into integer multiples of 180-bp units, resulting in a characteristic ladder on agarose gel electrophoresis. Figure 2B shows the typical DNA fragmentation when K562 cells were treated with compound **8** for 24 h. In addition, the Annexin V binding assay was performed to detect the transverse redistribution of plasma membrane phosphatidylserine, which is a hallmark of early apoptosis cells. Figure 2D shows the FACS histogram with dual parameters including Annexin V-FITC and PI. After being treated with the indicated concentration of compound **8** for 24 h, the results showed that only 5.25% cells were Annexin V positive when the concentration was 1 $\mu\text{g/mL}$, while the positive cells increased to 96.09% when the concentration was 100 $\mu\text{g/mL}$.

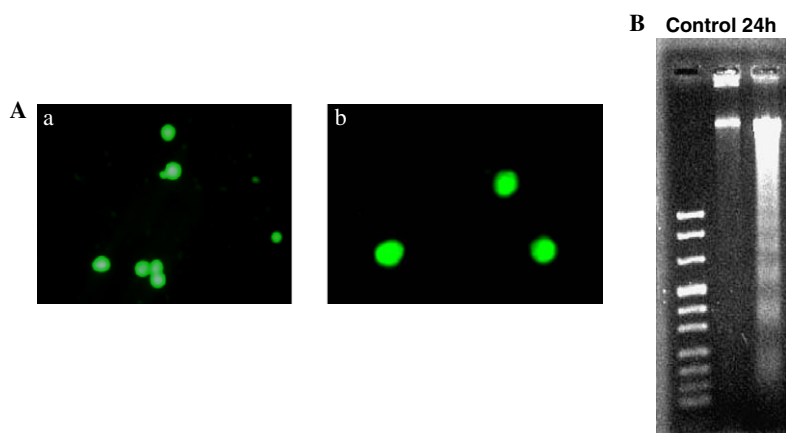


Figure 2. Effects of compound **8** on K562 cells. (A) Morphological changes of K562 cells. K562 cells were treated with 50 $\mu\text{g/mL}$ compound **8** for 24h(a), then, the cells were stained with AO (5 $\mu\text{g/mL}$) and examined by fluorescence microscopy. The cells without treatment were used as control (b). (B) DNA ladder assay. K562 cells were treated with 50 $\mu\text{g/mL}$ compound **8** for the indicated times. Apoptosis was evaluated by the induction of DNA fragmentation. (C) Cell cycle assay. K562 cells were treated with 50 $\mu\text{g/mL}$ compound **8** for the indicated times (a) and (b). K562 cells were treated at 1, 10, 50, and 100 $\mu\text{g/mL}$ for 24 h. Effects of compound **8** on cell cycle distribution in K562 cells were stained by propidium iodide and analyzed with the flow cytometric analysis. (D) Flow cytometric analysis of phosphatidylserine externalization and propidium iodide at 1, 10, 50, and 100 $\mu\text{g/mL}$ for 24 h.

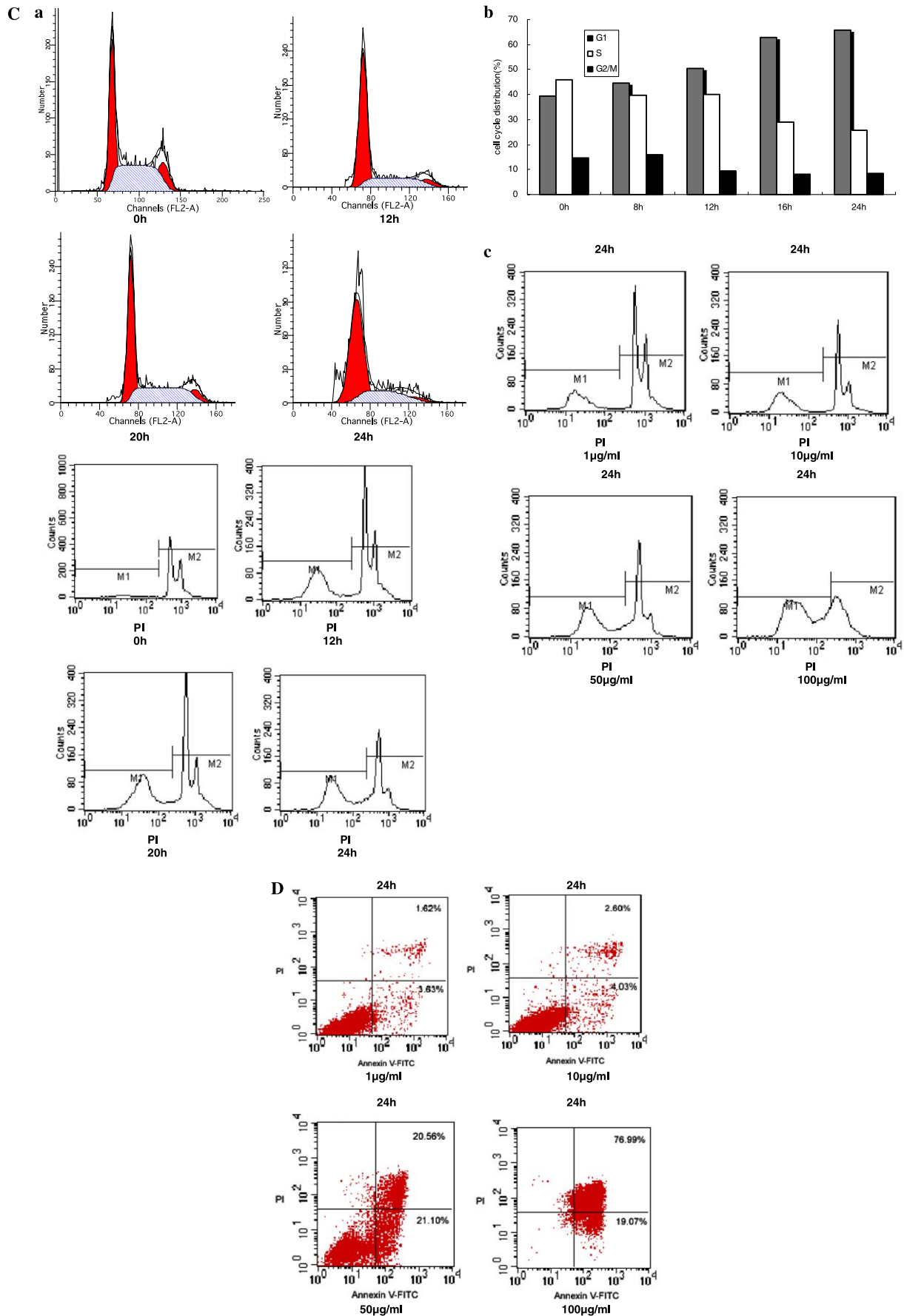


Figure 2. (continued)

As known, apoptosis is a process of cell suicide, characterized by specific morphological changes such as condensation of chromatin, blebbing of the plasma membrane and the appearance of apoptosis bodies, and biochemical properties involving fragmentation of chromatin. Furthermore, early in apoptosis, phosphatidylserine is translocated from the inner to outer surface of the plasma membrane which can be detected by Annexin V. Then early stage of apoptosis can be determined by Annexin V combined with PI staining. Taking the evidence mentioned above together, Compound **8** could indeed induce classical apoptosis in K562 cells. Moreover, a G_1 arrest was also observed with a time-dependence during this process. At the same time, a decrease of cells in both S and G_2/M phases, especially in S phase, was accompanied. For the lower the S-phase fraction, the slower the cell division, which indicates that compound **8** can slow down the growth of K562 cells, or even stop the cancer.¹⁴

2.3. Compound **8** induces activation of caspase-3, 8, and 9

Compound **8** induced the activation of caspase-3, caspase-8, and caspase-9 in the apoptotic process. Apoptosis is mainly brought about by activation of caspases, a protease family with unique substrate selectivity. As known, caspase-8 is involved in the death-receptor pathway, while caspase-9 mediates the mitochondrial pathway. Once activated, they can then activate downstream caspase-3, which finally causes DNA fragmentation. In the compound **8** induced apoptotic process, control cells displayed a minimal degree of caspase-3, 8, and 9 activity, in contrast, the activities of caspase-3, 8, and 9 increased dramatically in the treated cells after 24 h incubation. Therefore, the result shows that both death-receptors and mitochondria were involved in the process. The activation of the three caspases could be blocked by a caspase general inhibitor z-VAD-fmk, which is an irreversible inhibitor, a fluoromethyl ketone derived peptide.¹⁵ Different concentrations of inhibitors have been tried, 50 μ M had the best effect. However, not all the cells could be inhibited completely. The result here presented that key executors caspase-3, 8, and 9 mediated the apoptotic process partly. In addition, cells treated with 50 μ M compound **8** for 24 h exhibited typical apoptotic morphological changes other than the necrotic properties that appeared. Therefore, perhaps even another form of death was involved in this process. It is reported that a non-apoptotic form of cell death, which is mediated by caspase-9, has been discovered. The form of death was programmed, characterized by apoptotic morphology, but did not respond to inhibitors of apoptosis¹⁶ (Fig. 3).

2.4. Compound **8** induces the depolarization of mitochondria with the loss of MMP

When $\Delta\Psi_m$ of K562 cells was estimated using the probe DioC₆(3), a significant depolarization of mitochondria occurred. For the percentage of cells with lower fluorescence increased greatly (Fig. 4). During apoptosis, mitochondria suffer specific damages that result in loss of their function. Release of cytochrome *c*, the sole

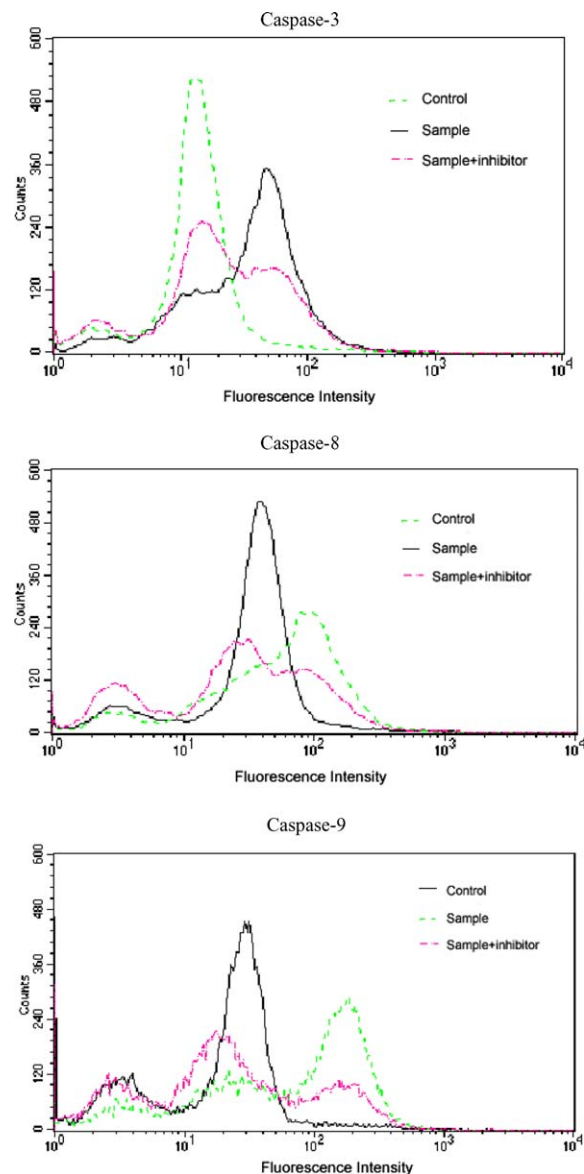


Figure 3. Caspase activity assay. Caspase activity changes among control K562 cells, cells treated with 50 μ M compound **8** and cells treated with both 50 μ M of compound **8** and general caspase inhibitor z-VAD-fmk (caspase-3 stained by FITC-DEVD-FMK, caspase-8 stained by FITC-IEDT-FMK, and caspase-9 stained by FITC-LEHD-FMK).

water-soluble component of the electron transfer chain, can potentially halt the electron transfer, leading to failure in maintaining the mitochondrial membrane potential. Our result here indicated that the $\Delta\Psi_m$ decreased and that compound **8** induced apoptosis is associated with mitochondria, which is consistent with the activation of caspase-9.⁶

2.5. Compound **8** induces the efflux of intracellular Ca^{2+} and the transient generation of ROS in K562 cells

Treatment with compound **8** rapidly enhanced the intracellular Ca^{2+} levels within the first 2 h (Fig. 5). Then the intensity of Fluo-3 fluorescence decreased slightly and reached a minimum at 4.5 h. After that, it increased dramatically, indicating that the elevation of Ca^{2+} concen-

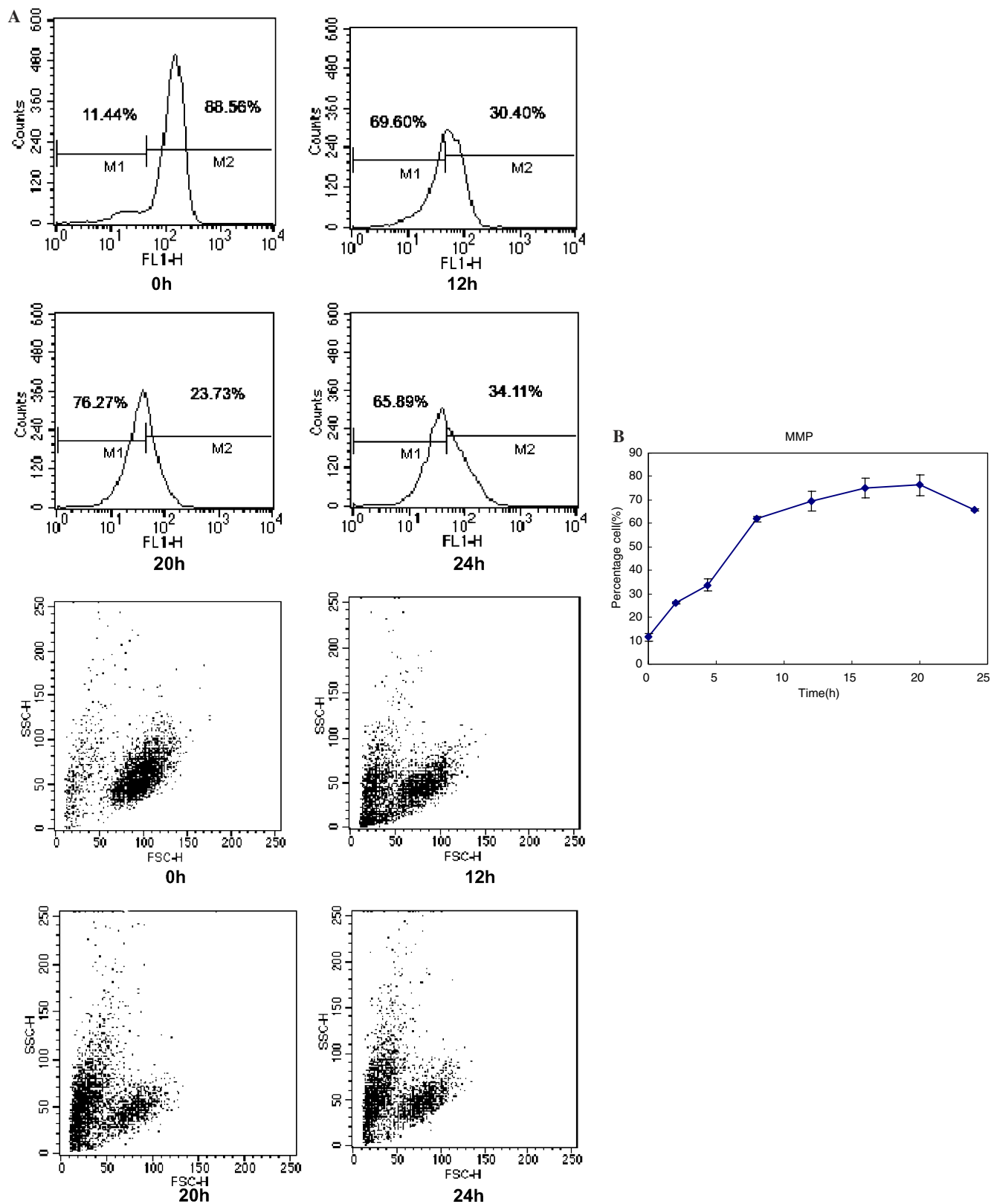


Figure 4. Time course analysis of MMP in the process of compound **8** induced apoptosis. K562 cells were treated with 50 $\mu\text{g/mL}$ compound **8** for the indicated times. The MMP changes were determined by DioC₆(3) fluorescence with FACS. (A) The result of FACS (FL1-H corresponds to DioC₆(3) fluorescence; FSC-H, cell granularity; SSC-H, cell size). (B) The percentage of cells that have lower DioC₆(3) fluorescence.

tration is an important initial step for compound **8** induced apoptosis. In addition, the generation of ROS was also involved in the process which was determined

by DCFH-DA fluorescence (Fig. 6). The percentage of cells with higher fluorescence reached a maximum at 3 h and then declined rapidly.

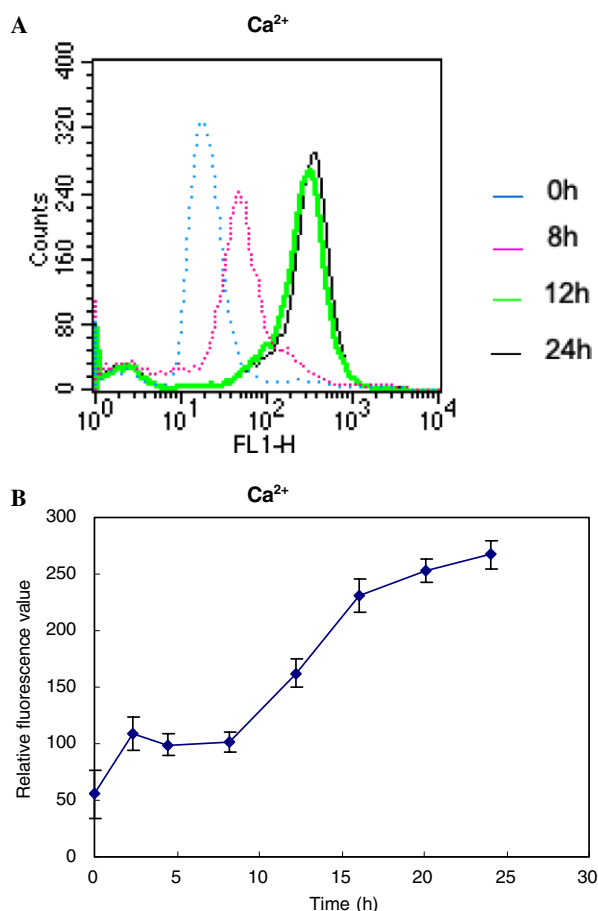


Figure 5. Effect of compound **8** on cytoplasmic Ca^{2+} concentration in K562 cells. (A) The result of FACS. (FL1-H corresponds to Fluo-3 fluorescence). (B) The time-dependent fluorescence activity of Fluo-3. K562 cells were treated with 50 $\mu\text{g}/\text{mL}$ compound **8** for the indicated times. Intracellular Ca^{2+} concentrations were determined in terms of the fluorescent activity of Fluo-3 by FACS analysis.

Ca^{2+} is a ubiquitous intracellular messenger, which mediates multiple signaling cascades that are critical for cell survival and apoptosis. It has been found that elevation in the cytosolic Ca^{2+} concentration can lead to apoptosis.^{17,18} ROS are known as intracellular second messengers at low concentrations and are able to activate transcription factors, such as AP-1. The burst of ROS in the cytosol might act as a mediator in apoptotic pathways and in turn act on MMP to influence mitochondrial function.¹⁹ In whole cell systems, the production of ROS and the collapse of $\Delta\Psi_m$ are both a cause and consequence of apoptosis.²⁰ In a mitochondrial-dependent apoptosis, mitochondria undergo what is referred to as the mitochondrial permeability transition (MPT), which has several consequences including the collapse of $\Delta\Psi_m$, Ca^{2+} release, and the generation of reactive oxygen species. MPT is controlled by a voltage- and Ca^{2+} -sensitive pore, PT pore, the opening of which is determined by several factors such as Ca^{2+} and $\Delta\Psi_m$.^{21–23} Based on the study, we speculate that compound **8** caused the accumulation of Ca^{2+} and ROS concentration in the early stage, accompanied by dissipation of $\Delta\Psi_m$. They interact to open the PT pore allowing for direct communication between the mito-

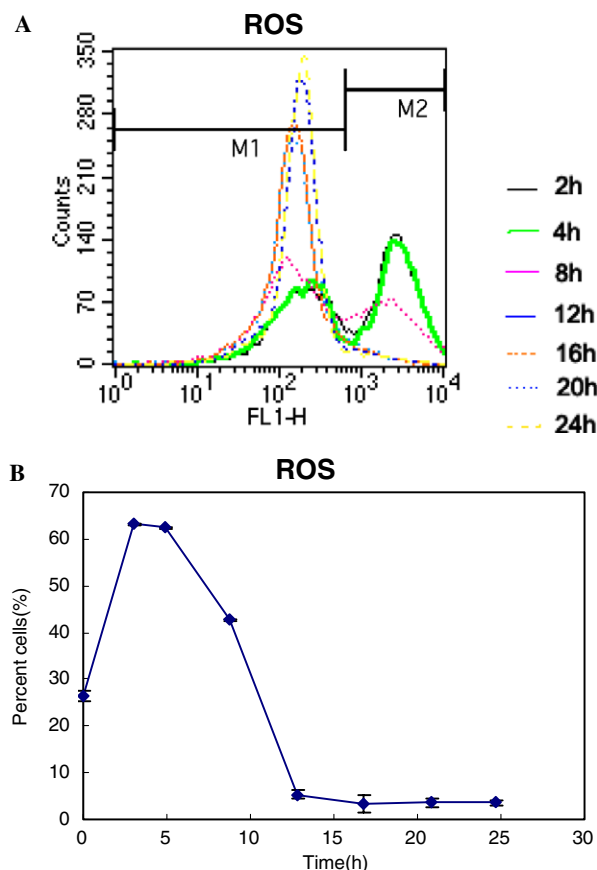


Figure 6. The generation of ROS was involved in compound **8** induced apoptosis. K562 cells were treated with 50 $\mu\text{g}/\text{mL}$ compound **8** for the indicated times. The ROS generation was determined in terms of DCFH-DA fluorescence by FACS analysis. (A) The result of FACS (FL1-H corresponds to DCFH-DA fluorescence). (B) The percentage of cells that have higher DCFH-DA fluorescence.

chondria and the surrounding environment. Therefore, an abrupt increase of Ca^{2+} , a transient peak of ROS, and the continuing loss of $\Delta\Psi_m$ were observed in the later stage.

As both death-receptor pathway and mitochondrial pathway are involved in the apoptotic process mentioned above, it can be conjectured that at the stimulus of compound **8**, death receptors at the surface of cells bind to their ligands. This oligomerization leads to activation of caspase-8 which then initiates a caspase cascade leading to cell death finally. At the same time, compound **8** can directly stimulate mitochondria, which causes the change of Ca^{2+} and ROS concentration and other proteins such as Bcl-2 protein family. Meanwhile, this process is also mediated by the change of Ca^{2+} and ROS concentration. These two pathways might be presented separately or exist for cross-talk.

3. Conclusions

In conclusion, the novel nitrogen heterocycle compounds can inhibit the proliferation of human CML cell line

K562, among which compound **8** has the best effect, with IC_{50} 20.83 $\mu\text{g/mL}$. Compound **8** caused cell cycle G_1 arrest and apoptosis in K562 cells. The apoptotic process was dependent not only on the activation of caspase-8, the mitochondrial pathway, but also on the activation of caspase-9, the death-receptor pathway, both of which finally activate caspase-3. However, another form of non-apoptotic death was also detected. In addition, the results revealed the associations among Ca^{2+} efflux, the generation of ROS, and the loss of $\Delta\Psi_m$. Compound **8** might be a potential chemopreventive agent for human chronic myelogenous leukemia. This study would encourage us to investigate the factors mediating the apoptotic process and to find function targets in order to synthesize more effective compounds by chemical modification. Furthermore, it might also provide a background mechanism for the introduction of this new type of promising therapeutic agent in the study for cancer chemotherapy.

4. Experimental

4.1. Cell culture

Human CML cell line K562 was purchased from Peking Union Medical College Hospital. The cells were cultured in RPIM 1640 medium (Cibco), with 10% fetal bovine serum (FBS) (Hyclone Laboratories Inc.), 100 IU/mL penicillin, and 100 $\mu\text{g/mL}$ streptomycin in humidified air at 37 °C with 5% CO_2 .

4.2. Materials

3-(4,5-dimethyl-thiazol-2-yl)-2,5-Diphenyl-tetrazolium bromide (MTT), propidium iodide (PI), Acridine orange (AO), 2',7'-dichlorodihydrofluorescein diacetate (DCFH-DA), Fluo-3, and 3',3'-dihexyloxacarbocyanine ($DiOC_6(3)$) were purchased from Sigma Chemical Co. Annexin V-FITC Apoptosis Detection Kit I and FITC-conjugated Antibody Reagent Set were from BD Biosciences Pharmingen. Caspase-3, 8, and 9 Detection Kit was purchased from Merck oncogene. Bax (D2D) PE, Bcl- x_L (H-5) PE phycoerythrin-conjugated, and normal mouse IgG $_1$ PE were from Santa Cruz Biotechnology Inc. CA.

4.3. Cell viability

The cells were suspended at a final concentration of 2×10^5 cells/mL and seeded in 96-well microtiter plates. Various concentrations of compound were added to each well in triplicate. After incubation for the indicated times, MTT assay was employed to measure cell viability. After treatment, the cells were incubated with MTT (5 mg/mL) for 4 h. The formazan precipitate was dissolved in 100 μL DMSO and the absorbance at 490 nm was measured by a Benchmark microplate reader (Molecular Devices Corporation).

4.4. Cytomorphology

The cells were directly observed under an inverted phase-contrast microscope (Leica DMIRB) and record-

ed with a Leica CCD camera (DC200). The nuclei were stained with AO (Acridine orange, 5 $\mu\text{g/mL}$) and examined by fluorescence microscopy (Leica DMIRB and MPS60, Leica Microsystems Wetzlar GmbH).

4.5. Flow cytometric analysis of cell cycle and apoptosis

Cells were fixed by 70% ethanol at –20 °C for at least 12 h. After two washes with phosphate-buffered solution (PBS), the cells were incubated in RNase A/PBS (1 mg/mL) at 37 °C for 30 min. Intracellular DNA was labeled with PI (50 $\mu\text{g/mL}$) and analyzed with a FACSCalibur fluorescence-activated cell sorter (FACS). The cell cycle profile was gained by analyzing 15,000 cells with ModFIT LT program (BD). Surface exposure of phosphatidylserine in apoptotic cells was measured by Annexin V-FITC/PI apoptosis detection kit I (BD Biosciences Pharmingen).

4.6. DNA fragmentation assay

The untreated and treated cells were harvested and lysed in 100 μL buffer [10 mM Tris–HCL (pH 7.4), 10 mM EDTA (pH 8.0), and 0.5% Triton X-100]. The supernatant was acquired through centrifugation at 16,000g for 5 min and then incubated with RNase A (10 mg/mL) at 37 °C for 1 h. Proteins were removed by incubation with Proteinase K (200 $\mu\text{g/mL}$) at 50 °C for 30 min. The lysate was added with 20 μL of 5 M NaCl and 120 μL of isopropanol. After deposition at –20 °C for 12 h, the precipitated DNA pellet was dissolved in Tris–acetate–EDTA buffer a 1.5 agarose gel, stained with ethidium bromide, and photographed under UV illumination.

4.7. Caspase assays

Cells induced by compound, a control culture without induction and a negative control with caspase inhibitor Z-VAD-FMK (1 $\mu\text{L/mL}$), were prepared. After 24 h, 300 μL each of the induced and control cultures was gained in tubes. One microliter of the caspase-3 fluorescent marker FITC-DEVD-FMK (caspase-3 Detection Kit, Merck), caspase-8 fluorescent marker FITC-IETD-FMK (caspase-8 Detection Kit, Merck), and caspase-9 fluorescent marker FITC-LEHD-FMK (caspase-9 Detection Kit, Merck) was added separately into each tube. After 1 h incubation in a 37 °C incubator with 5% CO_2 , the cells were centrifuged at 3000 rpm for 5 min. The supernatants were removed and the deposits were washed in 0.5 ml of wash buffer twice. Caspase-3, 8, and 9 were analyzed by a FACS.

4.8. Measurement of mitochondrial membrane potential

After treatment with compound, K562 cells were collected and washed twice with PBS. Resuspended cells in 0.5 mL PBS were incubated in the dark with 0.1 μM $DiOC_6(3)$ at 37 °C for 30 min, the cells were washed again and analyzed with a FACS.

4.9. Measurement of intracellular ROS generation

Intracellular ROS production was measured by using a fluorescent dye, DCFH-DA, which can be converted

to DCFH by esterases when the cells take it up. DCFH is reactive with ROS to give a new highly fluorescent compound, dichlorofluorescent, which can be analyzed with FACS. The treated cells were incubated with DCFH-DA (10 μ M) at 37 °C for 1 h and then measured with the FACS.

4.10. Analysis of intracellular Ca^{2+} concentration

The changes of intracellular Ca^{2+} concentration were determined by a fluorescent dye, Fluo-3. Cells were washed twice with RPMI 1640 medium and incubated with 5 M Fluo-3 at 37 °C for 30 min. Then, the cells were washed and analyzed with FACS.

4.11. Statistical analysis

One-way analysis of variance was performed to determine the significance between groups. A *P*-value of less than 0.05 ($P < 0.05$) was considered as statistically significant. All the figures shown in this article were obtained from at least three independent experiments with a similar pattern.

Acknowledgment

This work was supported by the National Natural Science Foundation of China (Grant No. 20472043).

References and notes

1. Steller, H. *Science* **1995**, 267, 1445.
2. Chris Bleackley, R.; Heibin, J. A. *Nat. Prod. Rep.* **2001**, 18, 431.
3. Alfons, L. *BioEssays* **2003**, 25, 888.
4. Nika, N. D.; Stanley, J. K. *Cell* **2004**, 116, 205.
5. Shi, Y. G. *Structure* **2002**, 10, 285.
6. Katja, C. Z.; Christine, B.; Douglas, R. G. *Pharmacol. Ther.* **2001**, 92, 57.
7. Bruno, A. *Mol. Cell. Biochem.* **2004**, 256/257, 141.
8. Wang, X. D. *Gene Dev.* **2001**, 15, 2922.
9. Reviews: (a) Nubbemeyer, U. *Top. Curr. Chem.* **2001**, 216, 125; (b) Maier, M. E. *Angew. Chem. Int. Ed.* **2000**, 39, 2073; (c) Evans, P. A.; Holmes, B. *Tetrahedron* **1991**, 47, 9131; Selected examples: (d) Lindström, U. M.; Somfai, P. *Chem. Eur. J.* **2001**, 7, 94; (e) Bieräugel, H.; Jansen, T. P.; Schoemaker, H. E.; Hiemstra, H.; van Maarseveen, J. H. *Org. Lett.* **2002**, 4, 2673; (f) Derrer, S.; Davies, J. E.; Holmes, A. B. *J. Chem. Soc., Perkin Trans. 1* **2000**, 2957; (g) Nicolaou, K. C.; Vourloumis, D.; Winssinger, N.; Baran, P. *Angew. Chem. Int. Ed.* **2000**, 39, 44; (h) Maier, M. E. *Angew. Chem. Int. Ed.* **2000**, 39, 2073.
10. (a) Taunton, J.; Collins, J. L.; Schreiber, S. L. *J. Am. Chem. Soc.* **1996**, 118, 10412; (b) Murray, P. J.; Kranz, M.; Ladlow, M.; Taylor, S.; Berst, F.; Holmes, A. B.; Keavey, K. N.; Jaxa-Chamiec, A.; Seale, P. W.; Stead, P.; Upton, R. J.; Croft, S. L.; Clegg, W.; Elsegood, M. R. *J. Bioorg. Med. Chem. Lett.* **2001**, 11, 773.
11. Yasuyuki, E.; Michihiro, O.; Masaaki, H.; Akiko, I.; Koichi, S. *J. Am. Chem. Soc.* **1996**, 118, 1841.
12. Alan, P. K.; Wang, S.; Ma, D.; Yao, J.; Shakeel, A.; Robert, I. G.; Krisztina, B.; Peter, A.; Shayan, M.; Nancy, E. L.; Peter, M. B. *J. Med. Chem.* **1997**, 40, 1316.
13. Yang, T.; Lin, C. X.; Fu, H.; Jiang, Y. Y.; Zhao, Y. F. *Org. Lett.* **2005**, 7, 4781.
14. Zi, X. L.; Agarwal, R. *Proc. Natl. Acad. Sci. U.S.A.* **1999**, 96, 7490.
15. Mohamed, A. E.; Zhu, Q.; Wang, Q.; Gulzar, W.; Altaf, A. W. *Int. J. Cancer* **2005**, 117, 409.
16. Kristen, M. C.; Nancy, B.; Mark, E. N.; George, L. *J. Cell Physiol.* **2005**, 205, 133.
17. Crompton, M. *Biochem. J.* **1999**, 34, 1233.
18. Liu, M. J.; Patrick, Y. Y.; Wang, Z.; Ricky, N. W. *Cancer Lett.* **2005**, 224, 229.
19. Li, P. F.; Dietz, R.; Von, H. R. *EMBO J.* **1999**, 18, 6027.
20. Blatt, N. B.; Glick, G. D. *Bioorg. Med. Chem.* **2001**, 9, 1371.
21. Kroemer, P. H.; Zamzami, N.; Susin, S. S. *Immunol. Today* **1997**, 18.
22. Zoratti, M.; Szabo, I. *Biochim. Biophys. Acta* **1995**, 1241, 139.
23. Kroemer, G.; Dallaporta, B.; Resche-Rigon, M. *Annu. Rev. Physiol.* **1998**, 60, 619.